FULL PAPER

Electric-Field-Assisted Nanostructuring of a Mott Insulator

By *Vincent Dubost, Tristan Cren, Cristian Vaju, Laurent Cario,* Benoit Corraze, Etienne Janod, François Debontridder,* and *Dimitri Roditchev**

Here, the first experimental evidence for a strong electromechanical coupling in the Mott insulator $GaTa_4Se_8$ that allows highly reproducible nanoscaled writing by means of scanning tunneling microscopy (STM) is reported. The local electric field across the STM junction is observed to have a threshold value above which the clean (100) surface of $GaTa_4Se_8$ becomes mechanically instable: at voltage biases >1.1 V, the surface suddenly inflates and comes in contact with the STM tip, resulting in nanometer-sized craters. The formed pattern can be indestructibly "read" by STM at a lower voltage bias, thus allowing 5 Tdots inch^{-2} dense writing/reading at room temperature. The discovery of the electromechanical coupling in $GaTa_4Se_8$ might give new clues in the understanding of the electric pulse induced resistive switching recently observed in this stoichiometric Mott insulator.

1. Introduction

Electric pulse induced resistive switching (EPIRS), which accounts for a nonvolatile change of resistance upon application of an electric pulse, shows a current burst of interest because of its possible applications in nonvolatile memory devices.[1] So far, three mechanisms, namely, joule heating, interfacial electronic injection, and ionic electromigration, are essentially evoked to explain the EPIRS phenomenon[1] encountered in materials such as NiO,[2] manganites,[3] and $SrTiO_3$,[4] respectively. However, a recently discovered EPIRS phenomenon in the non-centrosymmetric fragile Mott insulator $GaTa_4Se_8$[5] is not described by any of these mechanisms. Due to its peculiar crystalline and electronic structures, this clustered lacunar spinel compound lies on the verge of the metal–insulator transition, which makes it very sensitive to external parameters. Thus, $GaTa_4Se_8$ undergoes an insulator-to-metal and even superconducting transition under pressure.[6] More unexpectedly, electric pulses[5] induce an electronic phase separation on a nanometer scale in this compound and provoke an insulator to granular metal/superconductor transition.[7] While both pressure and electric field provoke an insulator–metal transition, it is not clear if the resulting metallic states are identical at the microscopic scale. In this Full Paper we report a scanning tunneling microscopy (STM) experiment performed on the clean (100) surface of $GaTa_4Se_8$; experimental evidence is given of a strong coupling, down to the nanoscale, between the electrical and mechanical properties in this material. We show that the surface of a $GaTa_4Se_8$ crystal becomes mechanically unstable upon the application of a local electric field across the STM junction, above a certain threshold. This strong electromechanical effect enables a nanoscale etching of the surface, which is used to create nanostructured patterns stable at room temperature; the density of these patterns could be as high as 5 Tdots inch^{-2}. Moreover, our discovery supports, in a complementary manner, a new EPIRS mechanism based on the Mott transition proposed for $GaTa_4Se_8$ in the work of Vaju et al.[5]

Our previous preliminary study revealed that pristine $GaTa_4Se_8$ crystals were hardly measurable via STM, while crystals that had undergone EPIRS prior to the measurement were much more suited for STM studies.[5] In that respect, in the present report we have focused on so-called weakly transited $GaTa_4Se_8$ crystals, which were prepared as follows: Firstly, four electric contacts were glued onto a small single pristine crystal (typical crystal size ~100–300 μm) of $GaTa_4Se_8$. Then, at a temperature $T = 77$ K, a series of electric pulses of increasing intensity was applied through the current leads while the conductance state was controlled via the voltage leads.[7] At this temperature, the fully transited crystals show a resistance change over several orders of magnitude[5] upon switching. However in the present study, in order to obtain weakly transited crystals, the series of pulses was stopped when the resistance of the sample after the pulse was found to be roughly half of its value in the pristine insulating state. The nonvolatile character of the transition was confirmed in both four-probe and two-probe configurations, thus, indicating its bulk nature. This weakly transited state remained stable at room temperature for several weeks. All the STM results described hereafter were obtained on such weakly transited crystals.

The weakly transited crystals were carefully oriented and glued on our STM sample holder and introduced into the ultrahigh

[*] Dr. L. Cario, Dr. C. Vaju, Dr. B. Corraze, Dr. E. Janod
Institut des Matériaux Jean Rouxel (IMN), Université de Nantes, CNRS
2 rue de la Houssinière, 44322 Nantes Cedex 3 (France)
E-mail: laurent.cario@cnrs-imn.fr
Dr. D. Roditchev, V. Dubost, Dr. T. Cren, Dr. F. Debontridder
Institut des Nanosciences de Paris (INSP), CNRS UMR 75-88
Université Paris 6 (UPMC)
140 rue de Lourmel, 75015 Paris (France)
E-mail: dimitri.roditchev@insp.jussieu.fr

DOI: 10.1002/adfm.200900208

vacuum (UHV) STM chamber (base pressure of 7×10^{-11} mbar, where 1 mbar = 100 Pa). Then, they were cleaved in situ along the (100) planes by using a hardened-steel blade. Electrochemically etched tungsten STM tips were thermally annealed under UHV up to 1300–1400 K by direct current heating before use, to remove oxide at the tip apex. The large-scale topographic STM images acquired on such in situ cleaved surfaces display large terraces, several hundred of nanometers wide (Fig. 1a). These terraces are notched by 0.5 nm deep trenches of various widths, all aligned in the same direction. The direction of the trenches can be related to the crystal structure of $GaTa_4Se_8$. Indeed, the crystal structure of the material[6,8] corresponds to a rocksalt-type packing of Ta_4Se_{16} clusters and $GaSe_4$ tetrahedra, sharing Se atoms. Hence, a cleavage parallel to (100) likely breaks Ta−Se bonds, exposing a slab where Ta_4Se_{16} clusters and $GaSe_4$ tetrahedra alternate. The thickness of such a slab is half the unit cell parameter, that is, 0.5 nm, a value that corresponds to the depth of the observed trenches. The surface space group is *p2mm* and the direction of the trenches corresponds to the [1-1] direction, parallel to the rows of $GaSe_4$ tetrahedra and Ta_4Se_{16} clusters (Fig. 1b). This kind of pattern, as well as its close relation to the crystal structure, is strong evidence of an important surface relaxation.[9] A magnified image of an atomically flat terrace is shown Figure 2a. Despite its disordered appearance, the surface has very low roughness, typically 100 pm. The self-correlation analysis allows a characteristic lateral size for the observed bumps to be estimated as roughly 3 nm. Despite numerous attempts, atomic-resolution imaging has not been achieved on this surface;[10] spatial inhomogeneities have been observed everywhere on the surface, and their overall pattern is reproducible from one sample to another.

The tunnelling junction was characterized by using current-versus-distance spectroscopy $I(Z)$. As the tip is retracted, the $I(Z)$ spectra display an exponential decay. Assuming a standard expression for the tunnelling current, $I(Z) = \exp(-2\kappa Z)$, where $\kappa = \sqrt{2mW/\hbar^2}$ and $m^* = m_e$, one obtains a high work function $W = 5.6 \pm 0.2$ eV, evidencing a clean vacuum tunneling junction.

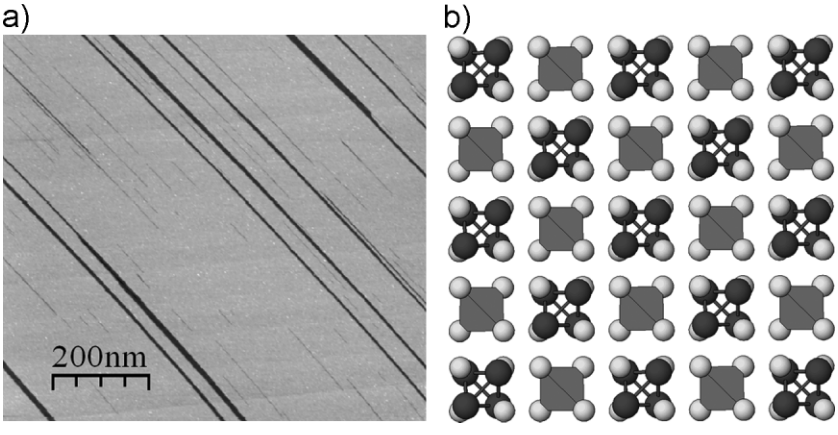

Figure 1. a) Topographic STM image ($V_{bias} = 0.71$ V, $I_T = 0.179$ nA) acquired on a cleaved surface of $GaTa_4Se_8$ under ultrahigh vacuum. b) Crystal structure of the (100) plane of $GaTa_4Se_8$ (Ta atoms: dark gray, Se atoms: light gray, $GaSe_4$ tetraedra: medium gray). The arrows indicate the crystallographic direction of the trenches.

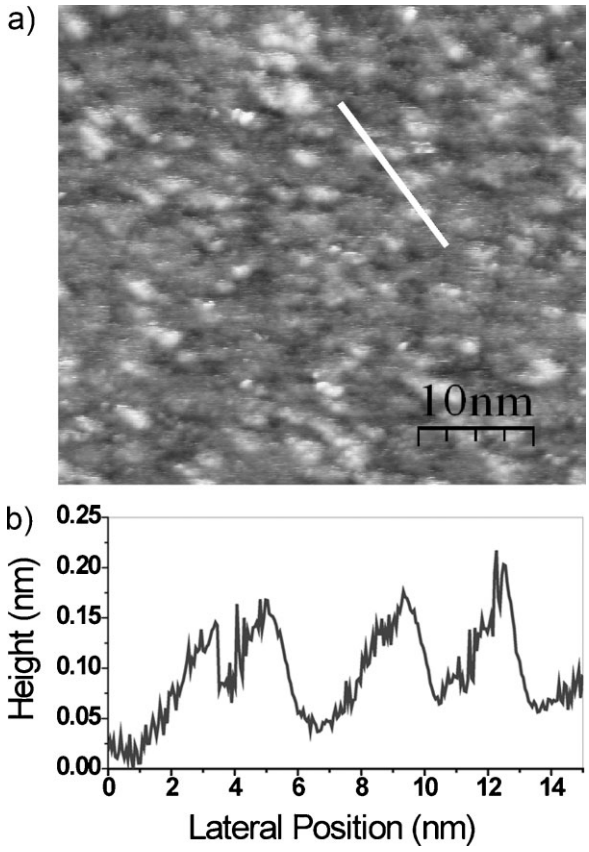

Figure 2. a) Small-scale topographic STM image ($V_{bias} = 0.80$ V, $I_T = 0.11$ nA), showing inhomogeneities with a characteristic size of ~3 nm. b) The topographic profile corresponding to the line in (a), which shows the 1 Å typical roughness of the surface.

2. Results and Discussion

The influence of voltage pulses was studied in the following manner. First, the tip position was regulated with a typical current set-point $I = 0.1$ nA for an applied voltage across the junction $V_{bias} = 0.7$ V. Then, the tip position was fixed by switching off the STM feedback loop, and a rectangular bias pulse was applied for the desired time. At the end of the pulse, the bias voltage was switched back to its initial value, and the STM feedback loop was switched on. While such pulses did not produce any effect at low biases, for bias pulses higher than 1.1 V, we systematically observed a sudden saturation of the STM current pre-amplifier. This is a clear signature of the appearance of a conducting link between the STM tip and the sample surface.[11] In order to evaluate the effect of the pulses on the surface, we performed constant current STM images of the perturbed region with a moderate $V_{bias} \approx 0.7$ V, at which value the tunneling junction always showed conventional behavior. The STM images revealed that the pulses created nanometer-scaled craters with a typical

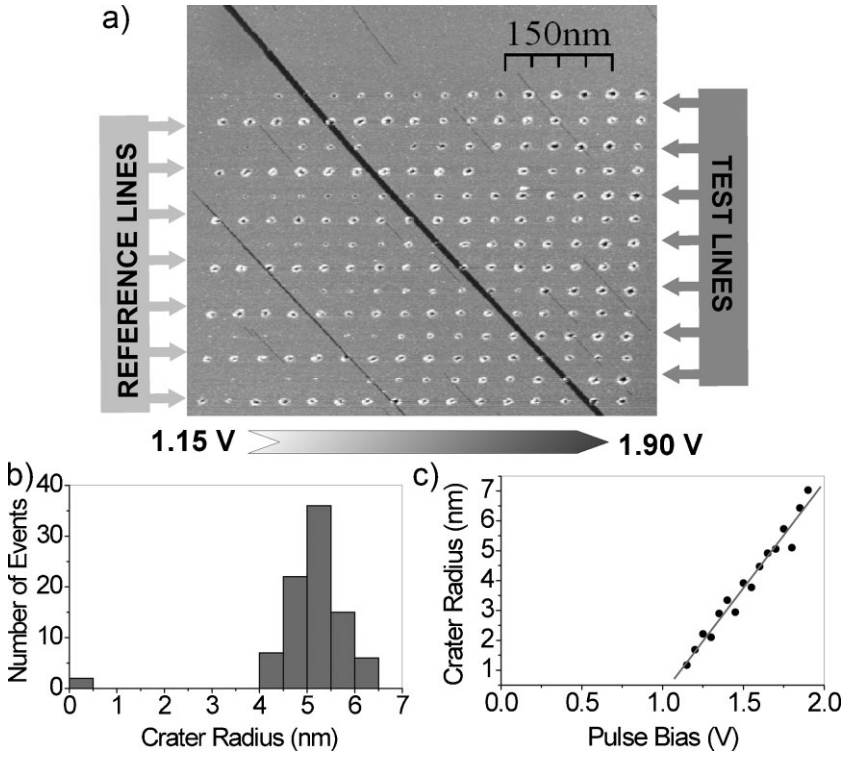

Figure 3. a) Topographic STM image ($V_{bias} = 0.71$ V, $I_T = 0.17$ nA) showing the effect of duration and voltage of the pulses. Reference grid lines are made with 100ms@1.6 V pulses. The test lines were done by varying the voltage pulse amplitude from 1.15 to 1.9 V from left to right while the pulse duration varies from 100 μs to 100 ms from bottom to top. b) A histogram showing the distribution of the crater radius of the reference grid. c) Dependence of the crater radius as a function of the pulse voltage: Dots represent the crater radius averaged with respect to the pulse duration; the solid line is a linear fit.

depth of 1 to 3 nm, as measured with respect to the unmodified surface (see Fig. 3a). Their inner structure displayed a pattern with a very reproducible shape, which we attributed to the footprint of the tip. This is quite similar to what Carrasco et al.[12] found in nanoindentation experiments on Au. The periphery of the crater is roughly circular. Such a peculiar crater shape is consistent with the formation of a tip–surface nanocontact upon bias pulses.

To analyze the effect of voltage pulses on crater size, we applied pulses on a grid varying both the pulse voltage and duration, as shown in Figure 3. The craters in the test lines (indicated in Fig. 3a) were created using 100 μs, 500 μs, 1 ms, 5 ms, 20 ms, 50 ms, and 100 ms pulse duration (from bottom to the top) and the pulse voltage was varied from +1.15 to +1.9 V by steps of 0.05 V (from left to right). On the other hand, all the craters of the reference grid lines (indicated on the left of Fig. 3a) were made with identical 100 ms pulses of 1.6 V. The reference lines were thus used to check the reproducibility of the crater creation.[13] The size distribution of the reference craters is surprisingly narrow, as the histogram in Figure 3b shows. One should note the very low rate of unsuccessful attempts, that is, missing crater (in Fig. 3a), which was of the order of 2%. The crater radius distribution nicely follows a Gaussian statistical form, with an average radius of 5.5 nm and a radius variation of about 10%. Looking at the test lines in Figure 3a, it can be directly seen that the pulse amplitude is a relevant parameter in the crater creation, while the pulse duration does not seem important, at least in the studied range. In Figure 3c, we have plotted the variation of the crater radius as a function of the pulse amplitude. The crater radius increases linearly with voltage pulse; an extrapolation to zero gives a voltage threshold of 1.1 V for the crater creation. We also checked the influence of the set point (i.e., of the tip-to-sample distance) on the crater formation. To do so, before applying the voltage pulse, we moved the tip towards the sample by a controlled distance ranging from 0 to 2 Å (keeping the feedback loop of the STM open). Within the studied range, we did not observe any significant dependence of the crater size and shape on the tip–sample distance. We argue that in the Mott insulator the screening is poor, and the electric field of the tip spreads well inside the material and consequently, it is not so sensitive to variations of a few angstroms of the tip–sample distance. Finally, we studied the influence of the sign of the voltage pulse but we did not find any significant difference between opposite voltage pulses.

Using the process described above, we were able to routinely create thousands of reproducible 10–15 nm wide craters at room temperature. In Figure 4, we give an example of such 10 nm resolution ''writing''. Remarkably, it was impossible to ''etch'' an entire region with such voltage pulses, that is, to create continuous ''cratered'' regions. In fact, the probability of creating a second crater in the vicinity of an existing one is very low for a separation distance

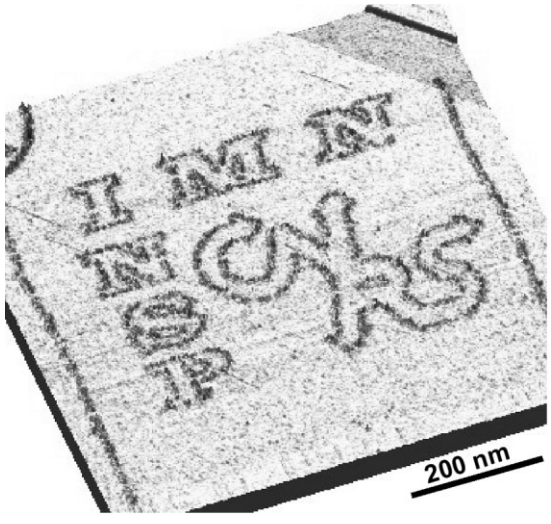

Figure 4. Topographic STM image ($V_{bias} = 0.758$ V, $I_T = 0.186$ nA) of a nanostructured pattern. The dots were done with 100 ms@1.6 V pulses. Note that a step of half the unit-cell height is clearly visible at the top of the image.

smaller than 10 nm. The origin of this effect is still unknown. Hence, with 100 ms@1.6 V pulses, the resolving power of such nanowriting is 10 nm, which corresponds to a density of about 5 Teradots inch^{-2}. This density can be further increased by optimizing the pulse voltages; the smallest reproducible craters were created with 1 ms@1.2 V pulses, giving a typical radius of 1 nm. Once created, these patterns are remarkably stable, and appear unmodified at room temperature for at least one week. Continuous scanning at voltages below the threshold value (1.1 V) does not affect the created structures.

Let us now address the possible mechanisms responsible for this surface nanostructuring. In fact, the nanoscale modification of a surface with an STM tip has been extensively studied in the past. Besides indentations on soft metals[12] or material deposition from the tips, different models for nanostructuring with STM have been proposed: mechanical contact, field evaporation, joule heating, electrochemical reactions. Electrochemical reactions, induced by the electric field of the tip on such materials as $SrRuO_3$, cuprates, gold, WSe_2, manganites,[14] are possible only in air because of the presence of a thin water film on the surface. In our case however, the crystals were cleaved under UHV and, consequently, the effect should be intrinsic to the clean surface of $GaTa_4Se_8$. The fact that the crater radius does not depend on the pulse duration while it varies linearly with the voltage pulse seems to exclude thermal effects as a possible origin. Field evaporation and local fusion[15] have also been proposed as possible origins for nanostructuring on phase-change materials; nevertheless, the voltage threshold for the field evaporation effect on clean surfaces is of the order of the binding energy, which corresponds to several volts. On silver chalcogenides (Ag_2S, Ag_2Se), the application of an electric field of the same order of magnitude as in our case, in STM as well as in nanobridge geometries, can generate a hole or a neck.[16] This mechanism involves the displacement of Ag^+ ions and is dependent on the sign of the electric field, which is not consistent with our results.

Therefore, none of the previously proposed mechanisms for nanostructuring the surface with an STM tip seems to apply in the case of $GaTa_4Se_8$. Conversely, all our observations for this compound are consistent with a mechanical instability of the surface upon the application of a local electric field. This surface inflation below the tip suggests the existence of an electromechanical coupling in $GaTa_4Se_8$. As the structure of $GaTa_4Se_8$ is noncentrosymmetric and compatible with piezoelectricity, a straightforward explanation of this phenomenon could be a piezoelectric response of the material. However, piezoelectricity is a linear, relation between the strain and the electric field, and hence dependent on pulse polarity, which is not consistent with our experimental findings. Therefore, at this stage, it is not possible to draw conclusions concerning the nature of the observed electromechanical coupling in $GaTa_4Se_8$. However, this finding might provide a new insight to the previously observed resistive switching. Indeed, $GaTa_4Se_8$ exhibits both a pressure- and an electric-pulse-induced insulator–metal transition. An electromechanical coupling that would convert the electric field in a kind of ''pressure effect'' might therefore be the missing link between the application of an electric pulse and the modification of the resistance state of $GaTa_4Se_8$.[5] In that respect, the electromechanical coupling evidenced in our experiments supports a new mechanism of the EPIRS phenomenon in $GaTa_4Se_8$, that is, an electric-pulse breakdown of the fragile Mott insulating state of this compound.

3. Conclusions

We have demonstrated that the UHV cleaved (100) surface of $GaTa_4Se_8$ becomes mechanically unstable upon the application of a local electric field. As a result, short voltage pulses above the threshold bias $V_{thershold} \approx 1.1$ V produce sharp holes in the surface. This process, which depends on neither sign nor pulse duration, can be used for nanostructuring the surface, allowing a stable pattern density up to 5 Teradot inch^{-2} at room temperature. This effect cannot be related to the mechanisms for nanoscale modifications of surfaces by STM reported until now. The most probable origin is linked to the presence of a strong electromechanical coupling in $GaTa_4Se_8$. In the near future, conducting-tip atomic force microscopy experiments will allow the bulging of the surface to be followed in a more direct way. Finally, the observed electromechanical coupling might give new clues to understanding the electric pulse induced resistive switching recently observed in this compound.

Acknowledgements

The authors thank Julie Martial at IMN for her help in samples' elaboration, and Jean-Charles Ricquier for his work on the figures. This work was supported by a Young Researcher grant (ANR-05-JCJC -0123-01) from the French Agence Nationale de la Recherche (to L.C., B.C., and E.J.)

Received: February 4, 2009
Revised: March 12, 2009
Published online: July 1, 2009

[1] R. Waser, M. Aono, *Nat. Mater.* **2007**, *6*, 833.
[2] D. C. Kim, S. Seo, S. E. Ahn, D. S. Suh, M. J. Lee, B. H. Park, I. K. Yoo, I. G. Baek, H. J. Kim, E. K. Yim, J. E. Lee, S. O. Park, H. S. Kim, U. I. Chung, J. T. Moon, B. I. Ryu, *Appl. Phys. Lett.* **2006**, *88*, 202 102.
[3] S. Q. Liu, N. J. Wu, A. Ignatiev, *Appl. Phys. Lett.* **2000**, *76*, 2749.
[4] K. Szot, W. Speier, G. Bihlmayer, R. Waser, *Nat. Mater.* **2006**, *5*, 312.
[5] C. Vaju, L. Cario, B. Corraze, E. Janod, V. Dubost, T. Cren, D. Roditchev, D. Braithwaite, O. Chauvet, *Adv. Mater.* **2008**, *20*, 2760.
[6] M. M. Abd-Elmeguid, B. Ni, D. I. Khomskii, R. Pocha, D. Johrendt, X. Wang, K. Syassen, *Phys. Rev. Lett.* **2004**, *93*, 126 403.
[7] C. Vaju, L. Cario, B. Corraze, E. Janod, V. Dubost, T. Cren, D. Roditchev, D. Braithwaite, O. Chauvet, *Microelectron. Eng.* **2008**, *85*, 2430.
[8] H. Ben Yaich, J. C. Jegaden, M. Potel, M. Sergent, A. K. Rastogi, R. Tournier, *J. Less-Common Met.* **1984**, *102*, 9.
[9] *Surface characterization*: At this stage of the study, the driving force for the surface relaxation phenomenon remains unknown; however, when cleaved in air, the samples do not show such relaxation.
[10] *STM resolution*: Note that our STM set-up has a resolution better than 1 pm as determined by atomic-resolution imaging on noble metal surfaces, like silver(111) obtained at room temperature.
[11] *Characterization of the effect*: Such a puzzling effect was observed uniquely on $GaTa_4Se_8$ crystals after an electric pulse. It was never observed in our STM set-up when studying Ag(111), Au(111), Si(111), Si(557), Pb/Si,

$NbSe_2$, highly oriented pyrolytic graphite (HOPG) samples with W, Au, Pt/Ir, Nb tips.

[12] E. Carrasco, M. A. Gonzalez, O. Rodriguez de la Fuente, J. M. Rojo, *Surf. Sci.* **2004**, *572*, 467.

[13] *Protocol modification*: Note that in some experiments we slightly modify the protocol: the tip was brought 2 Å closer to the surface after switching the feedback loop off. The only difference found is in the enhanced reproducibility of the crater formation, but there is no change in the aspect or in the size of the crater.

[14] C. C. You, N. V. Rystad, A. Borg, T. Tybell, *Appl. Surf. Sci.* **2007**, *253*, 4704. R. W. Li, T. Kanki, H. A. Tohyama, J. Zhang, H. Tanaka, A. Takagi, T. Matsumoto, T. J. Kawai, *J. Appl. Phys.* **2004**, *95*, 7091. Y. C. Fan, A. G. Fitzgerald, J. A. Cairns, *J. Vac. Sci Technol. B* **2000**, *18*, 2377. B. Jaeckel, Y. Gassenbauer, W. Jaegermann, Y. Tomm, *Surf. Sci.* **2005**, *597*, 65.

[15] R. Koning, O. Jusko, L. Koenders, *J. Vac. Sci Technol. B* **1996**, *14*, 48. C. S. Chang, W. B. Su, T. T. Tsong, *Phys. Rev. Lett.* **1994**, *72*, 574.

[16] a) Y. Utsigi, *Nature* **1990**, *347*, 747. b) K. Terabe, T. Hasegawa, T. Nakayama, M. Aono, *Nature* **2005**, *433*, 47.